

From Molecules to Supramolecular Structure: Self Assembling of Wirelike Poly(*p*-phenyleneethynylene)s

Dvora Perahia,^{*,†} Rakchart Traiphol,[†] and Uwe H. F. Bunz^{*,‡}

Department of Chemistry, Clemson University, and the Materials Research Program at Clemson University, Clemson, South Carolina 29634; and the Department of Chemistry and Biochemistry, The University of South Carolina, Columbia, South Carolina, 29208

Received September 6, 2000

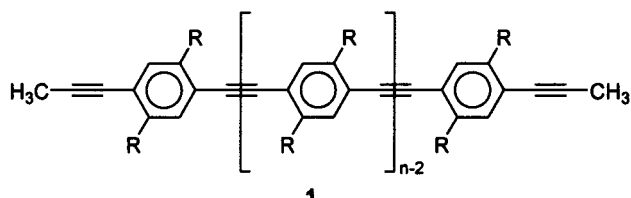
ABSTRACT: Supramolecular structures of lamellae folded into rodlike features were observed in thin films of dialkylpoly(*p*-phenyleneethynylene)s (*R* = 2-ethylhexyl, 2,5,5-trimethylhexyl, nonyl, dodecyl). The polymers have been melted onto oxidized silicon wafers and spontaneously wetted the wafers to form thin, micrometer thick films. These films were investigated by AFM microscopy and wide- and small-angle X-ray scattering. In all cases, spontaneous self-assembly of the PPEs occurs. The self-assembly process takes place on two length scales leading to lamellar ordering on the 2 nm scale and to rodlike structures on the 20–50 nm scale. The lamellar structure is observed by X-ray (all samples) where the large scale structure is detected by AFM. For high molecular weight PPE, the lamellae become rigid enough for the order to persist over larger domains, allowing the direct detection of the lamellae by AFM.

Introduction

In this contribution, we describe the supramolecular assembling of thin films of poly(*p*-phenyleneethynylene)s (PPEs, **1**)^{1–3} on the surface of oxidized single-crystal silicon wafers. These films have been investigated by wide- and small-angle X-ray scattering (WAXS and SAXS), and by atomic force microscopy (AFM). They are ordered on two length scales; i.e., lamellar structures fold into rodlike superstructures.

Conjugated polymers are organic semiconductors and as such of utmost importance in device applications ranging from “conventional” ones such as active layers in LEDs,⁴ photovoltaic cells,⁵ and thin film transistors⁶ to more advanced ones involving “molecular wires” in molecular electronics^{3,7} and nanomachinery. All of the above applications, however, from conventional to exotic do not take place in single, isolated molecules in vacuo but in condensed matter. Conjugated polymers⁸ show dramatic changes of optical, electronic and transport properties in the solid state, a consequence of both the tight interaction of extended chromophores and the (potential) planarization of the conjugated backbone into lamellar structures.⁹ As a consequence, the knowledge of the structure of thin organic polymer films on inorganic semiconductor supports is not only of fundamental importance and great scholarly interest but also a necessary prerequisite to build functional organic–inorganic hybrid devices. Of particular interest are cases where thin films of conjugated polymers on silicon or other conventional semiconductors self-assemble into nanoscopic structures, “nanopatterns”, a necessary prerequisite for the long-term goal of nanodevice construction. We have been interested in the synthesis and properties of PPEs (**1**) leading to device applications.^{8–10} Herein we present spontaneous supramolecular structures formed in thin PPE films on semiconductor-grade silicon wafers.

Table 1. Substituent Pattern, Molecular Weight, Polydispersity, Extended Length of the Backbones, and XRD Data of the PPEs **1**



PPE	R	<i>P_n</i>	<i>M_w/M_n</i>	ML (Å)	<i>d</i> (Å) (WAXS), bulk	<i>d</i> (Å) (WAXS), thin	<i>d</i> (Å) (SAXS), film
1a	ethylhexyl	35	2.5	270	12.8	12.1	ND ^a
1b	trimethylhexyl	23	1.8	180	18.1	17.3	199
1c	nonyl	168	4.0	1310	21.4	20.4	ND
1d	co-hexyl/dodecyl	79	4.8	610	22.0	21.5	ND
1e	dodecyl 2h	16	2.0	125	26.2	25.8	213
1e	dodecyl 3h	27	2.0	211	26.2	25.8	152, 194

^a ND: none detectable in the *q* range covered by our instrument.

Experimental Section

Alkyl-substituted PPEs, **1**, were synthesized as previously described.⁸ The different alkyl groups and corresponding molecular weights are given in Table 1. Five different PPE-derivatives (**1a–e**) have been investigated. The PPEs were melted into a film on top of an oxidized single-crystal silicon wafer. The samples were examined at room temperature by atomic force microscopy and by small and wide angle X-ray scattering. The X-ray studies were carried out on a Sintag XDS200 θ – θ powder diffractometer (Cu K α , λ = 1.54 Å; SAXS 40 kV, 20 nA, 6 h; WAXS 40 kV, 30 mA, 2 h). The θ – θ geometry indicates that the diffractometer operates in a reflection mode where the sample is stationary at the *x*–*y* plane and both detector and source move in the *Z* direction (no in plane scans can be carried out). The beam has a rectangular shape (2.0 mm × 0.8 mm; width at half-maximum). The experiments are carried out in a reflection mode to allow the study of the film on top of the silicon wafers. The data presented are scattering results on top of a reflectivity curve. This becomes most significant for the SAXS measurements where every peak is detected on top of the reflectivity as a shoulder of the main beam intensity. Since our instrument is not equipped with a monitor, we could not perform a quantitative deconvolution of the SAXS peaks, and

[†] Clemson University.

[‡] The University of South Carolina.

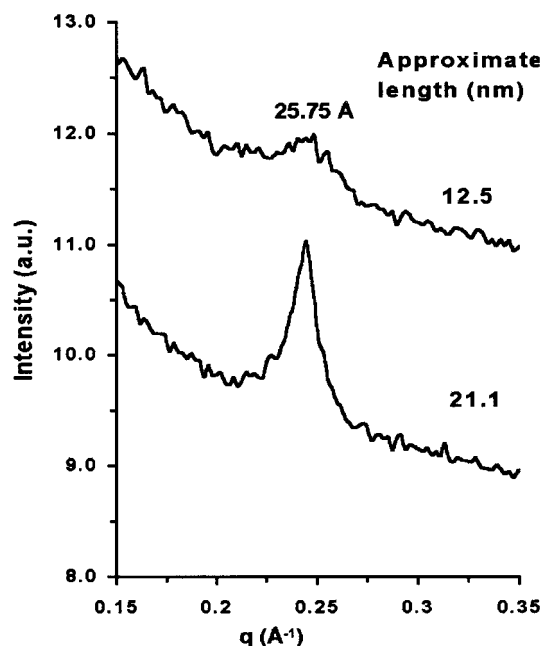


Figure 1. WAXS pattern of PPEs **1e** (R = dodecyl) recorded normal to the silicon surface, at two different degrees of polymerization: $P_n = 16$ and $P_n = 27$. The intensity in arbitrary units, where the total number of counts is divided by 10^5 , is plotted as a function of the momentum transfer q where $q = (4\pi/\lambda)\sin \theta$, θ is the incident angle, and λ is the X-ray wavelength.

our estimates for distances in large dimensions exhibit some error.

AFM measurements have been carried out on a digital multimode AFM in the tapping mode. Olympus cantilevers, with a spring constant of 42 N/m, resonating at 300 kHz, with different cross sections, have been used for all measurements. The strength of the tapping was varied to meet the needs of the specific sample. The tapping strength is given in units of volts, where the voltage is inversely proportional to the tapping

strength. Details are described in the captions of Figures 2 and 3. Samples were cast on oxidized single crystals in order to avoid roughness, which may affect the surface interactions.

Results and Discussion

The current study focuses on thin PPE films where the interfacial interactions are the significant force in aligning these wire-like molecules. Thin PPE films were made by melting PPE on oxidized silicon wafers and letting the melt spread spontaneously. Spreading, at elevated temperatures, with no external shear forces resulted in films of approximately $1\ \mu\text{m}$ thickness.

Structural measurements were carried out on several PPEs in both the wide- and the small-angle regimes. All PPEs studied show one clear peak in the wide-angle range, with a slightly smaller d value than the lamellar spacing recently reported for the bulk material^{8–10} and further confirmed in this study.^{9e,10} For bulk samples, many diffraction peaks are observed, which allowed an assignment of the solid-state structure of dialkyl PPEs to a lamellar model.^{9e,f,10} The values of the interlamellar spacing for films cast onto the surface, and values obtained from bulk samples, are summarized in Table 1. PPEs **1a–e** carrying different alkyl chains have been investigated. The wide-angle range consists of a few relatively narrow lines. While the interlamellar line is evident in the entire series, the other lines, observed in the bulk are either very weak or not detectable in our thin films. While spacings that correspond to the lamellar distance in the bulk are observed in the film, we cannot determine conclusively if the thin films are crystalline or amorphous.

Qualitatively, the distance between the lamellae increases with increasing chain length of the solubilizing substituent, R . The width of the peak, which is inversely proportional to the size of the coherently scattering domain, is independent of the size of the solubilizing substituent R . The peak width however decreases with

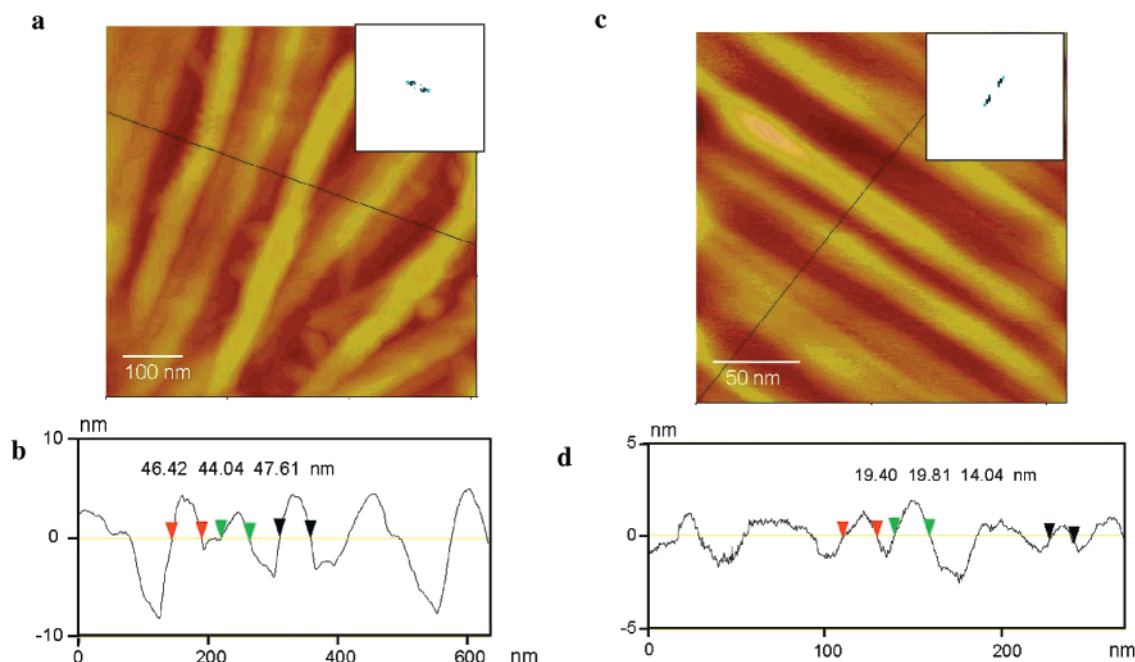


Figure 2. (a) AFM tapping mode height image of ethylhexyl PPE, **1a**, melted on an oxidized silicon wafer, measured at a set point of 0.787 V over a scan size of 609 nm. The top insert represents a two-dimensional Fourier transform with a peak average at 115 nm. (b) Height profile over the marked line in Figure 2(a). (c) AFM tapping mode height image of dodecyl PPE, **1e**, melted on an oxidized silicon wafer, measured at a set point of 0.863 V over a scan size of 211 nm. The top insert represents a two-dimensional Fourier transform with a peak average of 36 nm. (d) Height profile over the line marked in Figure 2(c).

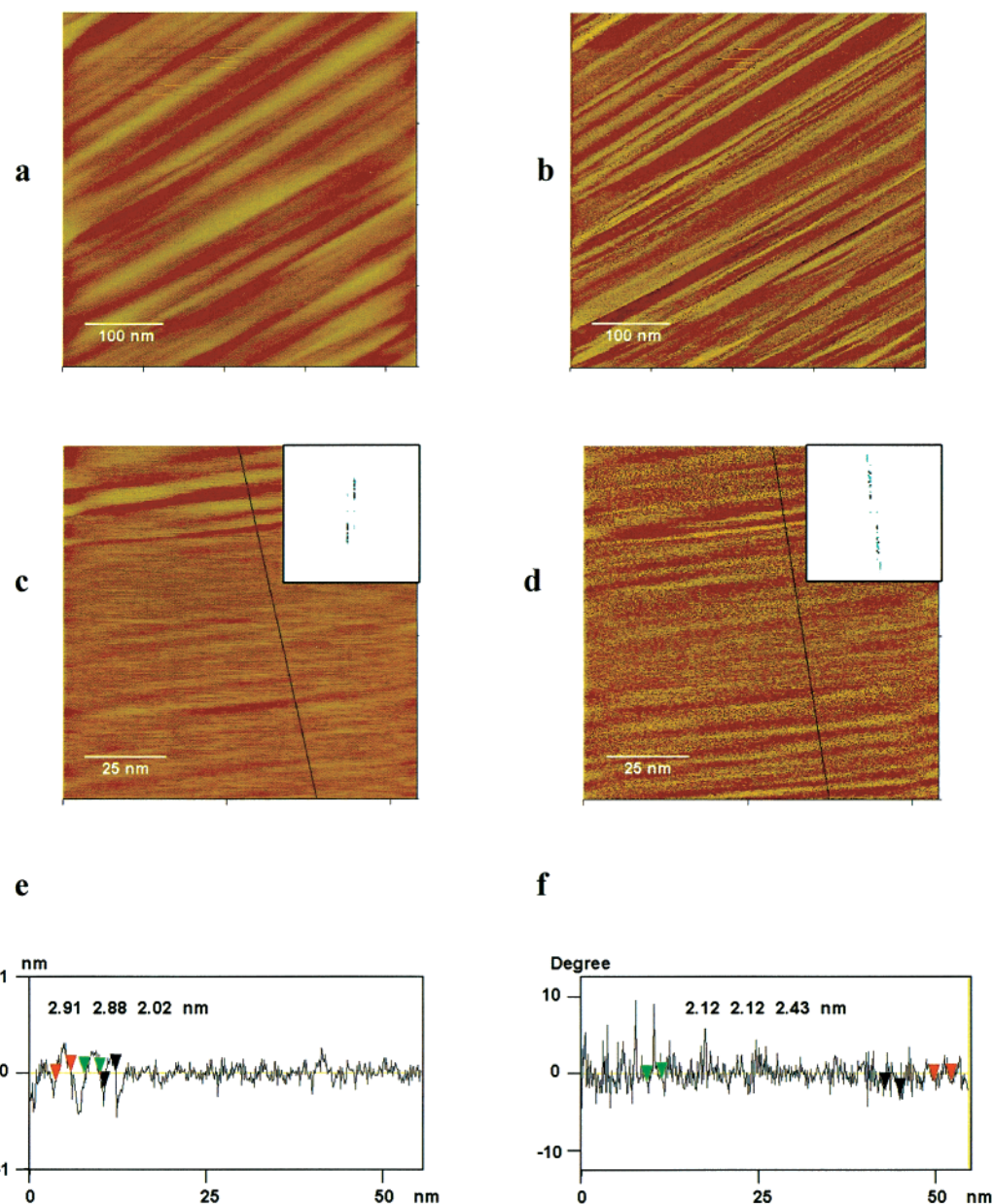


Figure 3. (a) AFM tapping mode height image of nonyl PPE, **1c**, melted on an oxidized silicon wafer, measured at a set point of 0.436 V. (b) Corresponding phase image. (c) Image similar to part a, with a scan size of 54.2 nm and set point of 0.338 V. (d) Phase image corresponding to that shown in part c. (e, f) Height and phase profiles along the lines marked on the images at (c) and (d), respectively.

increasing degree of polymerization (P_n), as can be seen in Figure 1 for PPE **1e** (R = dodecyl) for P_n = 16 and 27. The top curve corresponds to **1e** with a P_n of 16 units and the bottom one corresponds to a polymer **1e**, with a P_n of 27. While the position of the peak does not change, its width decreases dramatically, indicating that the lamellar ordering persists over a larger domain. This is in good agreement with the assumption that longer (rigid) rods pack more efficiently. To determine the long-range order in thin films of PPEs **1**, small-angle X-ray scattering was performed. All samples show one or two extremely broad SAXS peaks (Table 1) in the range of 13–21 nm, which corresponds to some of the features observed in the AFM and will be discussed in that context. While all samples have shown broad lines, we have reported only the numbers for samples that had an error of less than $\sim 10\%$. The SAXS lines are very broad, suggesting either an amorphous nature of the

sample or very small coherently scattering domains. While our setup does not allow deconvolution of the lines, the inherent nature of the system, forming a mesh of rods rather than continuous films, dictates the broadness of the lines. The nature of crystallization of polymers has been the topic of numerous studies. Long-range order with a periodicity of hundreds of angstroms has been observed in different polymers. It has been attributed either to alternating crystalline and amorphous domains or to long-range imperfections of the lattice.¹²

Self-assembly of conjugated oligomers¹¹ and polymers^{1–3} on surfaces is at the heart of the emerging field of molecular electronics. To further analyze the assemblies of PPEs, tapping mode AFM studies in both height and phase modes have been carried out. The height mode is sensitive to the morphology of the surface while the phase mode provides further information on

the viscoelastic properties of the film.

Figures 2 and 3 exhibit AFM images of thin PPE films, which reveal spontaneous self-association of PPE into rodlike structures. Both, PPEs with branched and with linear side chains form similar patterns. Figure 2a (tapping mode) shows a height image of PPE **1b** and Figure 2c displays an analogous image obtained for **1e**. Both PPEs spontaneously form rodlike superstructures. The rod diameter for **1a** (height profile, Figure 2b) is approximately 45 nm. A two-dimensional Fourier transform reveals an intense peak that corresponds to an average periodicity of 115 nm. This periodicity corresponds to the average distance between centers of two rods.

Figure 2c presents the tapping mode height image of PPE **1e**. Cylinders with a cross section of approximately 19 nm are observed. The SAXS data of the same sample consist of a broad peak at 21.3 nm. Within the accuracy of the AFM measurements (including the finite size of the tip) the values obtained from the broad X-ray peaks are in close agreement. The two-dimensional Fourier transform in the insert revealed a peak with average dimensions of 36 nm, corresponding to the average spacing between cylinders. Note that while we do show a direct cross section of the images, the values quoted for the size of the rods are from the Fourier transform analysis. This eliminates some of the inaccuracy, which may arise from the finite dimensions of the AFM tips. Combining the X-ray and AFM data suggests that these PPE derivatives form a supramolecular structure where layers of PPE are forming large cylindrical aggregates.

The patterns obtained by phase mode AFM have fully followed those of the height mode. No further distinctions between amorphous and crystalline domains have been observed on the length scale, which corresponds to the SAXS dimensions.

All examined PPEs exhibit supramolecular structures, similar to the lamellar packing observed in the bulk. The uniformity as well as the organization varies as a function of P_n . The X-ray line width analysis suggests that with increasing P_n of the PPE, the order persists over a larger length scale. As a consequence it was of interest to determine the influence of P_n on the spontaneous ordering of the polymer chains in thin films. Indeed when imaging PPE **1c** ($P_n = 168$, R = nonyl), the AFM measurement revealed both lamellar and rodlike structures, as shown in Figure 3. Figure 3, parts a and b, corresponds to height and phase mode images. Cylindrical aggregates, similar to those observed in the other PPEs, had formed. While the height image provides the topography of the surface, the phase mode is sensitive to the viscoelastic properties of the polymer film. From the phase mode it becomes obvious that there are "soft" and "hard" regions oriented on the surface. Further magnification reveals (Figure 3, parts c and d, height and phase images, respectively) repeating distances of approximately 21 Å in both modes. Similar distances are detected by the Fourier transforms (insets). The observed spacing of 21 Å can be attributed to the wingspan of the two nonyl chains attached to one benzene ring in the repeating unit of **1c**. This distance corresponds very well to the lamellar spacing obtained from bulk and thin film XRD data of **1c**! The soft and hard segments observed in the phase contrast picture of **1c** (Figure 3c,d) thus correspond to the alkyl chains (soft) and the conjugated backbone (hard) of **1c** respectively. As a consequence we see an ordering on two

different length scales, which correspond to the formation of lamellae, and an ordering of packages of these lamellae into the rodlike domains. Both lamellae and rods are clearly visible in the AFM images. It is known that PPE derivatives can form superstructures and Thünemann and Schnablegger have discovered that ester-substituted PPEs form mesoscopic arrays,¹³ while Müllen and Rabe demonstrated that PPEs form nanoribbons on surfaces.¹ The self-assembled structures in thin-film preparations of PPEs we see here are a third type of supramolecular arrangement, hitherto not described for dialkyl-PPEs. While different crystallization morphologies of polymers have shown periodicity on several length scales, the PPE films do not segregate into macroscopically amorphous and crystalline regimes, nor do we observe long-range imperfections of a lattice.

In conclusion, we have shown that PPEs self-assemble from the melt into rodlike/lamellar structures. These rodlike aggregates consist of lamellar arrangements previously observed in the bulk. As the molecular weight increases, the lamellae become stiffer and the long-range order becomes more pronounced. In this case (**1c**), the hard and soft parts of the PPE, viz. alkyl chains and conjugated backbones, can be discerned. With these experiments, we have established that PPEs spontaneously form superstructures on two different length scales and that irrespective of the nature of their solubilizing substituents or their P_n . Our future studies will address the nature of the ordering of PPEs on different length scales. Structural studies from ultrathin films of 10 nm to several micrometers will be carried out. We will explore the self-assembly of PPE as a function of the interaction of the polymer with the solid support. Different substrates such as mica, HOPG, glass, and gold will be examined. In addition, we will determine the influence of P_n on the mode of self-assembly in a more rigorous fashion.

Acknowledgment. U.H.F.B. is a Camille Dreyfus Teacher-Scholar (2000–2004) and thanks the National Science Foundation (CHE 9814118) and the Petroleum Research Funds for generous financial support. D.P. thanks Clemson University for startup funds. R.T. acknowledges the generous support of the Thai Government. We thank Dr. L. Kloppenburg for providing samples of polymer **1**.

References and Notes

- (1) Independent of us, Rabe and Müllen have examined the self-assembly of dihexyl-PPE on surfaces utilizing STM microscopy. See: Samori, P.; Severin, N.; Müllen, K.; Rabe, J. P.; *Adv. Mater.* **2000**, *12*, 579. Samori, P.; Francke, V.; Müllen, K.; Rabe, J. P. *Chem.—Eur. J.* **1999**, *5*, 5312. Samori, P.; Sikharulidze, I.; Francke, V.; Müllen, K.; Rabe, J. P. *Nanotechnology* **1999**, *10*, 77. Samori, P.; Francke, V.; Müllen, K.; Rabe, J. P. *Thin Solid Films* **1998**, *336*, 13.
- (2) For the self-assembly of defined phenyleneethynylene oligomers, see: Zehner, R. W.; Parsons, B. F.; Hsung, R. P.; Sita, L. R. *Langmuir* **1999**, *15*, 1121. Dhirani, A. A.; Zehner, R. W.; Hsung, R. P.; Guyot-Sionnest, P.; Sita, L. R. *J. Am. Chem. Soc.* **1996**, *118*, 3319.
- (3) Self-assembly of phenyleneethynylene oligomers: Bumm, L. A.; Arnold, J. J.; Cygan, M. T.; Dunbar, T. D.; Burgin, T. P.; Jones, L.; Allara, D. L.; Tour, J. M.; Weiss, P. S. *Science* **1996**, *271*, 1705.
- (4) Kraft, A.; Grimsdale, A. C.; Holmes, A. B. *Angew. Chem.* **1998**, *37*, 402.
- (5) Nanos, J. I.; Kampf, J. W.; Curtis, M. D. *Chem. Mater.* **1995**, *7*, 2232. Curtis, M. D.; Cheng, H. T.; Nanos, J. I.; Nazri, G. A. *Macromolecules* **1998**, *31*, 205. Kobel, W.; Kiess, H.; Egli, M. *Synth. Met.* **1988**, *22*, 265. Haddon, R. C.; Siegrist, T.;

- Fleming, R. M.; Bridenbaugh, P. M.; Laudise, R. A. *J. Mater. Chem.* **1995**, *5*, 1719.
- (6) Yu, G.; Gao, J.; Hummelen, J. C.; Wudl, F.; Heeger, A. J. *Science* **1995**, *270*, 1789.
- (7) Lindsey, J. S. *New. J. Chem.* **1991**, *15*, 153. Mirkin, C. A.; Ratner, M. A. *Annu. Rev. Phys. Chem.* **1992**, *43*, 719. Reed, M. A. *Proc. IEE* **1999**, *87*, 652.
- (8) Bunz, U. H. F. *Chem. Rev.* **2000**, *100*, 1605. Kloppenburg, L.; Jones, D.; Bunz, U. H. F. *Macromolecules* **1999**, *32*, 4194. Kloppenburg, L.; Song, D.; Bunz, U. H. F. *J. Am. Chem. Soc.* **1998**, *120*, 7973.
- (9) For aggregation and solid-state behavior of PPEs, see: (a) Halkyard, C. E.; Rampey, M. E.; Kloppenburg, L.; Studer-Martinez, S. L.; Bunz, U. H. F. *Macromolecules* **1998**, *32*, 8655. (b) Fiesel, R.; Halkyard, C. E.; Rampey, M. E.; Kloppenburg, L.; Studer-Martinez, S. L.; Scherf, U.; Bunz, U. H. F. *Macromol. Rapid Commun.* **1999**, *20*, 105. (c) Miteva, T.; Palmer, L.; Kloppenburg, L.; Neher, D.; Bunz, U. H. F. *Macromolecules* **2000**, *33*, 652. (d) Pschirer, N. G.; Bunz, U. H. F. *Macromolecules* **2000**, *33*, 3961. (e) Bunz, U. H. F.; Enkelmann, V.; Kloppenburg, L.; Jones, D.; Shimizu, K. D.; Claridge, J. B.; zur Loye, H.-C.; Lieser, G. *Chem. Mater.* **1999**, *11*, 1416. (f) Kloppenburg, L.; Jones, D.; Claridge, J. B.; zur Loye, H.-C.; Bunz, U. H. F. *Macromolecules* **1999**, *32*, 4460.
- (10) Ofer, D.; Swager, T. M.; Wrighton, M. S. *Chem. Mater.* **1995**, *7*, 418. Weder, C.; Wrighton, M. S. *Macromolecules* **1996**, *29*, 5157.
- (11) Müllen, K.; Wegner, G. Eds. *Electronic Materials: The Oligomer Approach*; Wiley-VCH: Weinheim, Germany, 1998.
- (12) Mendelkern, L. *Crystallization of Polymers*; McGraw-Hill Book Company: New York, 1964.
- (13) Thünemann, A. F.; Ruppelt, D. *Langmuir* **2000**, *16*, 3221. Thünemann, A. F. *Adv. Mater.* **1999**, *11*, 127. Schnablegger, H.; Antonietti, M.; Göltner, C.; Hartmann, J.; Colfen, H.; Samori, P.; Rabe, J. P.; Häger, H.; Heitz, W. *J. Colloid Interface Sci.* **1999**, *212*, 24.

MA0015469